

See discussions, stats, and author profiles for this publication at: <https://www.researchgate.net/publication/228869689>

# THE RCS ATTITUDE CONTROLLER FOR THE EXO-ATMOSPHERIC AND GUIDED ENTRY PHASES OF THE MARS SCIENCE LABORATORY

Article · January 2010

CITATIONS

10

READS

1,302

3 authors, including:



[Paul B Brugarolas](#)

California Institute of Technology

39 PUBLICATIONS 428 CITATIONS

[SEE PROFILE](#)



[Edward Wong](#)

21 PUBLICATIONS 334 CITATIONS

[SEE PROFILE](#)

# THE RCS ATTITUDE CONTROLLER FOR THE EXO-ATMOSPHERIC AND GUIDED ENTRY PHASES OF THE MARS SCIENCE LABORATORY

Paul B. Brugarolas<sup>(1)</sup>, A. Miguel San Martin<sup>(2)</sup>, Edward C. Wong<sup>(3)</sup>

*Jet Propulsion Laboratory, California Institute of Technology  
4800 Oak Grove Dr., Pasadena, CA, 91109 (USA)*

<sup>(1)</sup> Email: Paul.Brugarolas@jpl.nasa.gov

<sup>(2)</sup> Email: Alejandro.M.Sanmartin@jpl.nasa.gov

<sup>(3)</sup> Email: Edward.C.Wong@jpl.nasa.gov

## ABSTRACT

This paper describes the RCS 3-axis attitude control system for the exo-atmospheric and guided entry phases of the Mars Science Laboratory. The controller is formulated as three independent channels in the control frame, which is nominally aligned with the stability frame. Each channel has a feedforward and a feedback path. The feedforward path enables fast response to large bank slews. The feedback path stabilizes the vehicle angle of attack and sideslip around its trim position, and tracks bank commands. The performance of this design is demonstrated via simulation.

## 1. INTRODUCTION

The Mars Science Laboratory (MSL) is the next NASA rover mission to Mars. It will launch in 2011 and deliver a ~900 kg mobile science laboratory, a rover named “Curiosity”, to the surface of Mars. MSL aims to deliver this rover within a ~20 km landing circular region. MSL uses a guided atmospheric entry capsule to achieve this targeting performance. The entry capsule guidance, navigation and control system employs a set of ejectable balance masses, a descent inertial measurement unit (DIIMU), and a propulsive reaction control system (RCS). The ejectable balance masses shift the capsule center of mass enabling generation of a lift vector during the atmospheric phase. A guidance law that controls this lift vector through banking maneuvers corrects for down-track and cross-track errors. A navigation filter integrates the DIMU measurements to estimate the position and attitude of the capsule. The positional information is used by the guidance law. The attitude information is used by the attitude controller to track bank commands and stabilize the angle of attack and sideslip angle. The attitude controller generates torque commands that get implemented through the propulsive RCS system. This paper represents an update to work presented in [1].

## 2. THE MSL ENTRY CAPSULE

The MSL Entry Capsule is about 5 m in diameter and 3 meters in height. Figure 1 shows the elements used for attitude control. The propulsive RCS system is composed of 4 thruster pods with two thrusters each. The cruise balance masses (2), and the entry balance masses (6). The cruise balance masses are ejected after the entry capsule has been despun. They serve the purpose to generate a cg offset such that the capsule will have an L/D of .2 at mach 24. The entry balance masses are ejected right before the opening of the parachute to eliminate the cg offset. Six masses ejected over a period of few seconds enable a slow correction of the trim angle of attack.

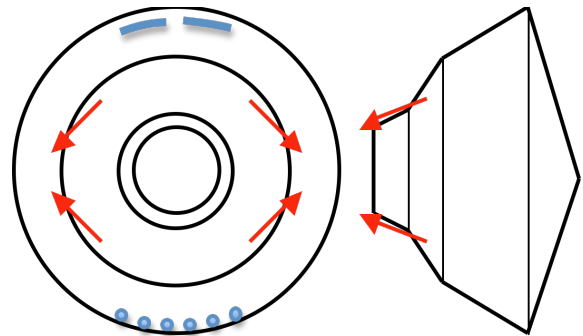


Fig. 1. The MSL Entry Capsule diagram indicating the RCS thruster's directions, the cruise balance masses (2), and the entry balance masses (6). Not to scale.

## 3. THE EXO-ATMOSPHERIC PHASE

The exo-atmospheric phase starts after separation from the Cruise stage and it last until the capsule enters the Martian atmosphere. During this phase the attitude controller will de-spin the capsule, turn to the predicted desired entry attitude, and hold that attitude. This phase lasts about 9 minutes. The exo-atmospheric phase control function diagram is shown in figure 2.

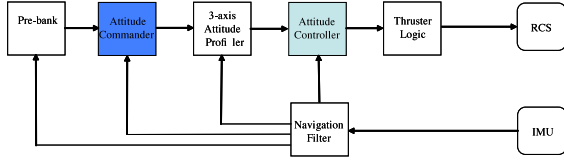


Fig. 2. Exo-atmospheric phase functional diagram.

The Attitude Commander block generates the desired attitude in two steps: A pitch rotation by the current predicted trim angle of attack; and a roll rotation by the desired initial bank angle, denoted as Pre-bank. Then 3-Axis Attitude Profiler generates the profile to take the entry capsule to that state. In doing so, it first nulls the angular rates and then it profiles a turn to the desired attitude. The Attitude Controller takes state information from the onboard Navigation Filter and the desired attitude from the 3-axis attitude profiler to generate the control errors. Then, it calculates the desired torques to zero the control errors. The Attitude Controller is a gain scheduled controller. The parameters are read from a parameter table which is indexed by the estimated atmospheric relative speed. The attitude controller will be further described in a later section. The Thruster Logic block provides a pulse-width-modulation implementation of the attitude controller desired torques.

#### 4. THE GUIDED ENTRY PHASE

The guided entry phase starts when the sensed acceleration reaches a given threshold. It finishes at parachute deploy at about mach 2. This phase lasts 2-3 minutes. The guided entry phase control function diagram is shown in figure 3.

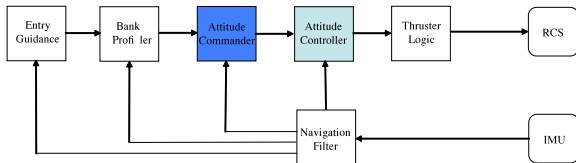


Fig. 3. Guided entry phase functional diagram.

During the entry phase, the Entry Guidance algorithm, which is derived from the Apollo command module final phase guidance algorithm and adapted to Mars entry, generates bank angle commands to control range-to-go and cross-range errors by adjusting the drag acceleration. [3]. When the cross-range errors exceed a given threshold the Entry Guidance algorithm will command a bank reversal. These reversals are large turns and therefore are profiled by the Bank Profiler, which plans a single axis accelerate-coast-decelerate attitude maneuver.

#### 5. THE ATTITUDE CONTROLLER

The entry capsule approximates a biconic vehicle. During the entry phase a CG-offset is used to create a lift to drag (L/D) ratio of approximately 0.24, which leads to a trim angle of attack of about -15.5 degrees at entry interface and varies slightly over time. The Entry Controller calculations are performed in a Control Frame, which is defined as a non-orthogonal frame depicted in Figure 4. The yaw (x-axis) and pitch (y-axis) correspond to eigenvectors of the aerodynamic oscillatory modes. The roll (z-axis) corresponds to the bank angle. This definition allows deadband settings around the dynamic variables of interest. Yaw and pitch deadbands are sized for rate damping of oscillatory modes. Bank deadband is sized for guidance performance.

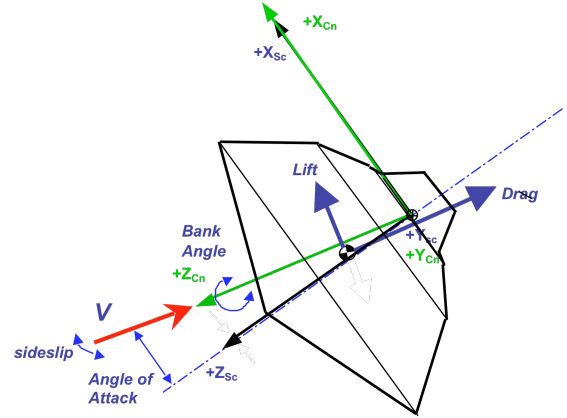


Fig. 4. Control Frame

This Control Frame is time varying since the vehicle's trim angle of attack varies over the trajectory. The predicted trim sideslip angle is nearly zero. These angles are derived from the MSL aerodynamic database developed by NASA's Langley Research Center [9]. Uncertainty in the predicted values needs to be accounted in choosing the attitude deadbands. The Viking project observed a 2 degree discrepancy between the predicted and actual angles of attack values [6] for both flights. In addition, the aerodynamics oscillatory mode frequency (short period, dutch roll) changes over the trajectory. The separation of the lateral and longitudinal aerodynamics, in conjunction with formulating the control problem in the Control Frame, enables the parameterization of the Entry Controller as three independent channels.

The structure of the controller for each channel has a feedback and a feedforward path. The feedforward path is used to achieve fast profiled maneuvers for large

turns. The feedback path is used to stabilize the plant. The feedback path is formulated as a phase plane controller with attitude and rate deadbands to minimize fuel usage. It is shown in figure 7. The attitude and rate errors are computed relative to the deadbands. Crossing the deadband engages the feedback gradually and therefore it is expected that the errors will surpass the deadbands. When the errors cross the attitude deadbands, a PD controller (dashed blue zone) is engaged. If the error crosses the rate deadbands, a D controller (solid green) is engaged. These enable to shape the frequency response of the controller. If the errors were to grow further, more the PD and D controllers will saturate and the behavior will be equivalent to a bang-bang controller (light shaded region)

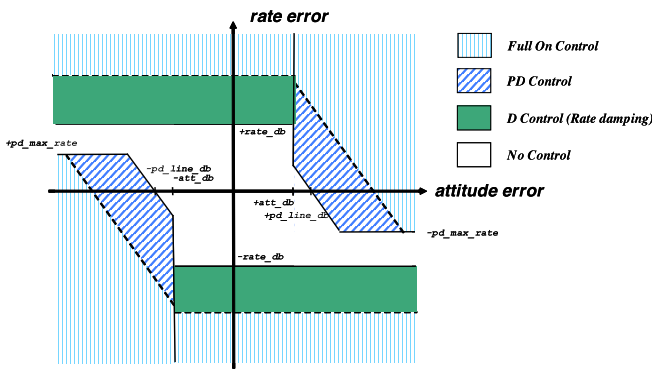


Fig. 5. Feedback path controller

The controller gains and deadbands are tabulated for different flight regimes and different events. During the exo-atmospheric phase, the attitude deadbands are set large in order to minimize fuel during limit cycling. Just before entry, the attitude deadbands are tightened up to reduce disturbance effects. During the entry phase, the attitude deadbands are set large and the rate deadbands small. This enables the feedback to behave primarily as a rate control. It provides both energy damping and robustness against knowledge errors in the predicted trim angle of attack. Both of the Viking vehicles trimmed at about 2 degrees higher negative angles than predicted [6]. Error in the predicted trim angle of attack is an important factor in the selection of the attitude deadbands when trying to minimize the fuel usage. Attitude deadbands need to be large enough to accommodate for trim prediction errors. Too small attitude deadbands in face of prediction errors will cause the controller to fight the actual trim angle of attack and result in large fuel consumption. For the same reason, the Viking landers flew a rate damping controller during the entry phase [6]. For MSL, the attitude deadbands are tightened up again before parachute deploy to reduce the initial attitude error and the subsequent dynamic disturbance during parachute

deployment.

In addition, a modification was introduced in the bank channel controller to react to large errors. It was observed that large persistent roll disturbances during bank reversals could cause large bank errors, which in turn could cause the guidance law to fall behind. It was recognized that in such cases, the controller could maximize its roll torque capability to fight the disturbance by giving up coordinated turns and commanding a pure roll torque.

## 6. SIMULATION AND DISCUSSION

This section shows a detail simulation example. The simulation was executed in the Control Analysis Simulation Testbed (CAST) which is a JPL developed computer simulation testbed for EDL. This testbed has models for the environment (gravity, aerodynamics, etc.) and for the spacecraft dynamics, sensors (IMU) and actuators (RCS). In addition, it calls the Guidance, Navigation, and Control (GN&C) algorithms as implemented in the actual flight software. First, we will describe the behavior during the exo-atmospheric phase. Section 6.1 describes the spin-down, turn-to-entry, and the exo-atmospheric attitude hold periods. Then, we will show the atmospheric phase in section 6.2.

### 6.1 Exoatmospheric Phase

Before any GN&C activities start, a train of RCS thruster firing is fired to warm up the RCS thrusters. Since the MSL cruise stage is a spinner. Once the entry capsule separates from the cruise stage, the entry capsule will remain spinning at about 12 deg/s. The first activity is to spindown the capsule and then turn to the desired entry attitude. The desired entry attitude consists of the predicted trim angle of attack and sideslip angle at contact with the Mars atmosphere, and a predicted initial bank angle derived to be consistent with the reference trajectory implemented in the Guidance algorithm.

Figure 6 shows the GNC mode versus time. This mode provides information on the on-going GN&C activities. The simulation was set to start at time equal to 1000 s. Before any GN&C activities start, a train of RCS thruster firing is fired to warm up the RCS thrusters (~ 20 s). Then, we spin-down (~ 6 s), and perform the turn-to-entry attitude maneuver (~ 14 s). Then we enter into the exo-atmospheric attitude hold phase (~ 500 s).

As mentioned earlier, large turns are profiled using the feedforward path. So, during the spindown and turn to entry will be profiled by the three axis attitude profiler. The attitude profiler will generate a profile angular

accelerations. Then the attitude controller will use that desired angular accelerations to calculate the desired feedforward torque. In addition, the feedback path of the controller will evaluate the attitude and rate errors against their deadbands. It will generate a feedback desired torque commands to keep these errors with the deadbands ( $\sim 2$  deg). Then, the RCS thruster logic implements the desired torques through pulse width modulation of the 8 RCS thrusters. Figure 7 shows the capsule attitude rates. Figure 8 and 9 show the attitude and attitude rate errors respectively. Figure 10 shows the total commanded torque and the feedforward torque. Figure 11 shows the commanded on-time durations to the RCS thrusters to implement the desired torque. Figure 12 shows the cumulative fuel used during this phase.

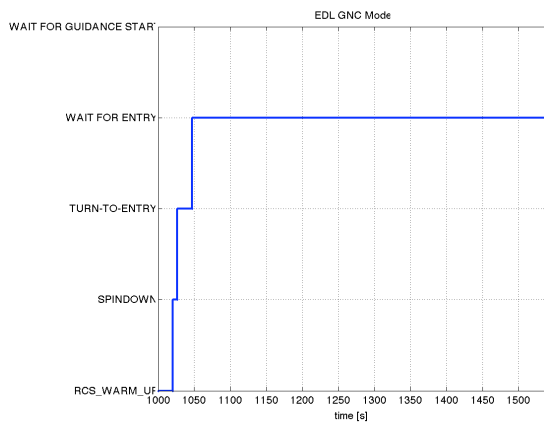


Figure 6. GNC Mode

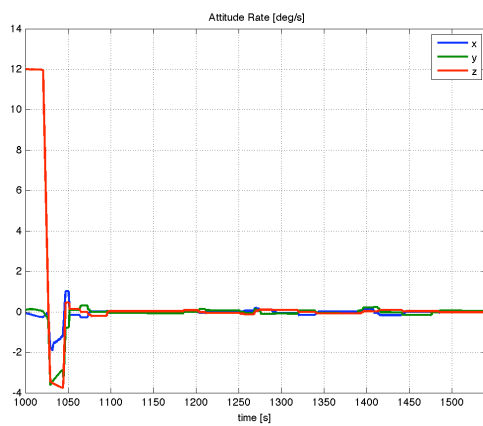


Figure 7. Capsule Rates.

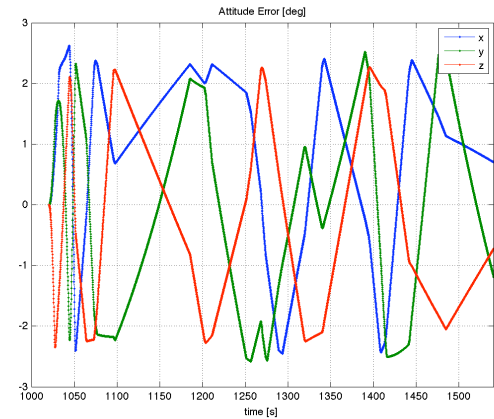


Figure 8. Attitude Errors

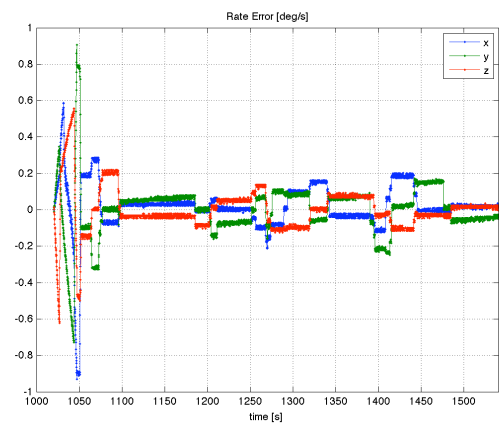


Figure 9. Attitude Rate Errors

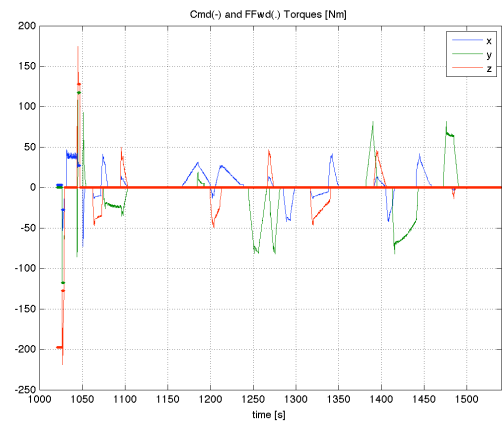


Figure 10. Commanded (-) and Feedforward (.) Torques

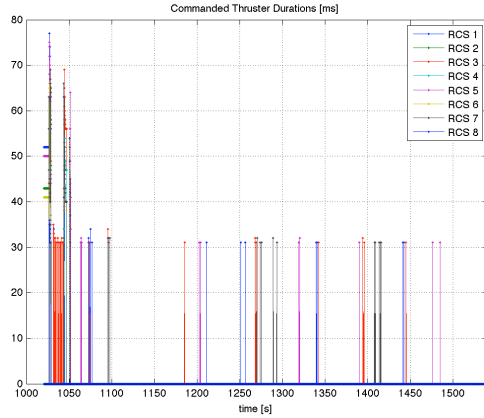


Figure 11. Commanded RCS Thruster durations.

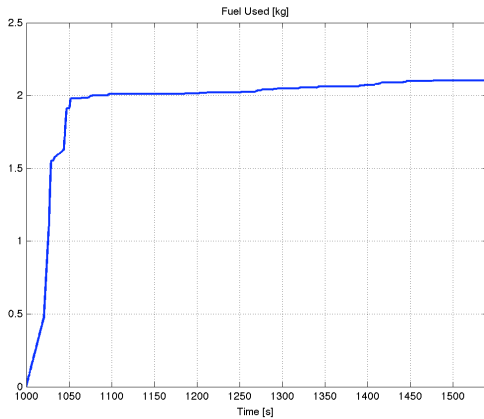


Figure 12. Fuel Used

## 6.2 Atmospheric Phase

The activities happening during the atmospheric phase are summarized in the EDL GNC mode, Figure 13. It starts at the *Wait for Guidance start* mode, where it waits until the sensed drag acceleration reaches a given threshold. At this point the Entry Guidance Range Control (RC) algorithm was called for the first time and generated its first bank angle command. The bank profiler will then profile a turn to take the bank angle from the pre-bank used during the exo-atmospheric phase to the new bank command, denoted as *RC Slew to Cmd Bank* mode. Then, it goes into *RC Track*, where the guidance algorithm tracks the downrange errors. When the cross-range errors get too large, it commands a bank reversal and the mode toggles to *RC Bank Reversal*. When the heading alignment (HA) phase starts, the bank profiler plans a turn to the first heading alignment bank angle, as *HA Slew to Cmd Bank*, and goes into *HA Track*. Before the chute opens a roll slew is performed to point the radar antennas to the ground, denoted as *SS Slew to Radar Att.* (where SS stands for *Straighten-up-fly-right Slew*). At the same time the

CG-offset is removed by ejecting 6 balance masses. Once the slew is complete, it goes into *SS Wait for Chute*, where it waits for the right conditions to open the parachute. When these conditions are met the entry attitude controller is disabled and the GNC mode goes into *Settle Chute Transients*. Figure 14 shows the bank angle time histories. It illustrates the bank profiles during the slews and bank reversals. Figure 15 shows the predicted and actual angles of attack. It shows a small mismatch between the predicted and the actual. Figure 16 shows the sideslip angle. Both angle and attack and sideslip angle shows aerodynamic induced oscillations. Figure 17 shows the actual spacecraft rates. Figure 18 and 19 show the attitude and rate errors. Figure 20 and 21 shows the attitude control desired torques and the commanded RCS thruster durations. Figure 22 shows the cumulative fuel consumption since the start of the exoatmospheric phase.

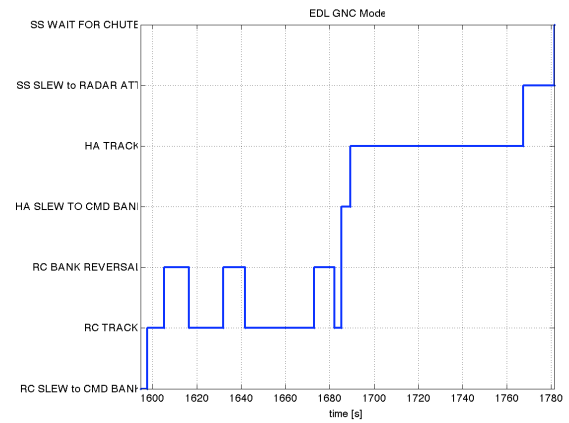


Figure 13. GNC Mode

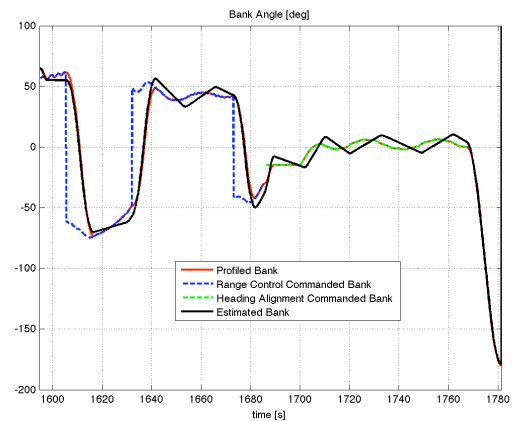


Figure 14. Bank angle.

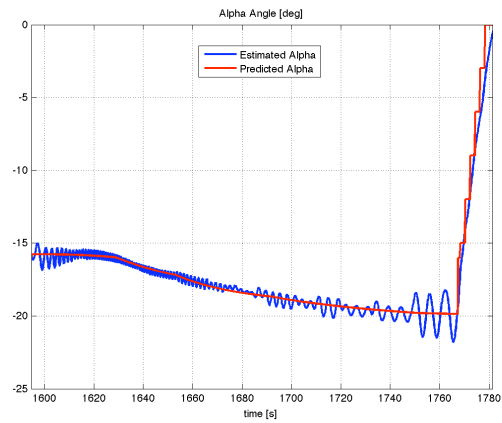


Figure 15. Angle of Attack

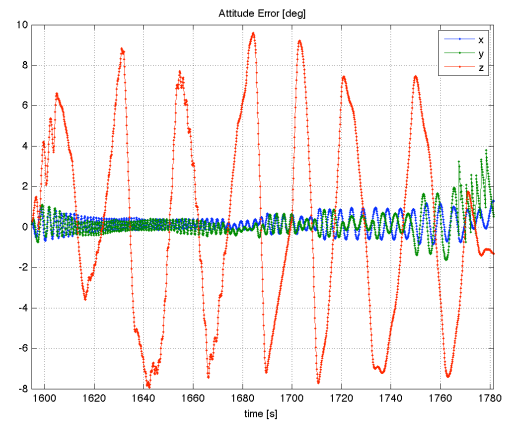


Figure 18. Attitude Errors

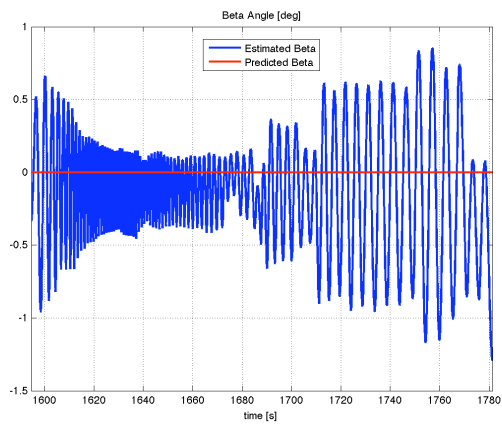


Figure 16. Sideslip angle

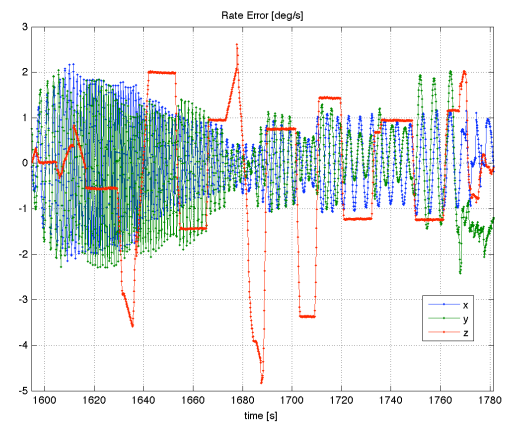


Figure 19. Attitude Rate Errors

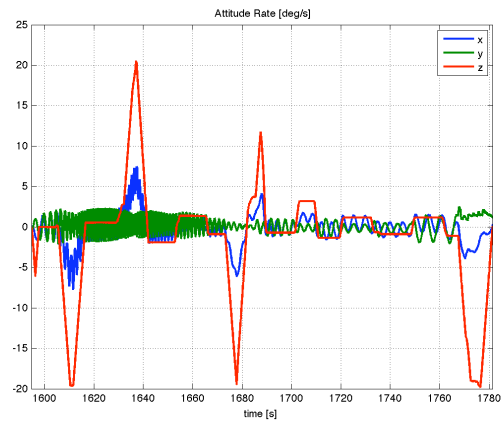


Figure 17. Capsule Rates

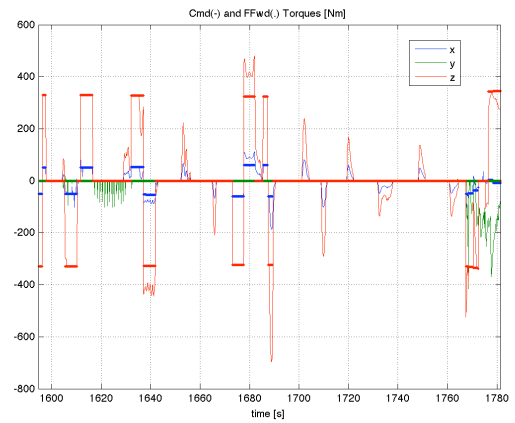


Figure 20. Commanded (-) and Feedforward (.) Torques



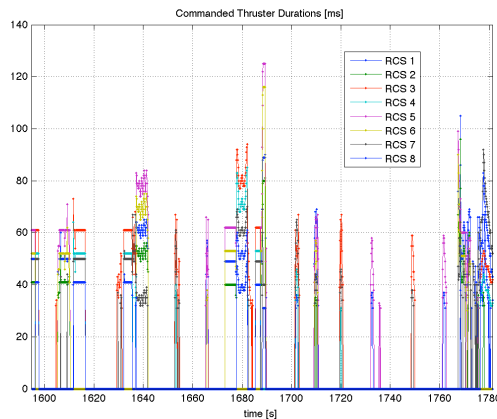


Figure 21. Commanded RCS Thruster durations.

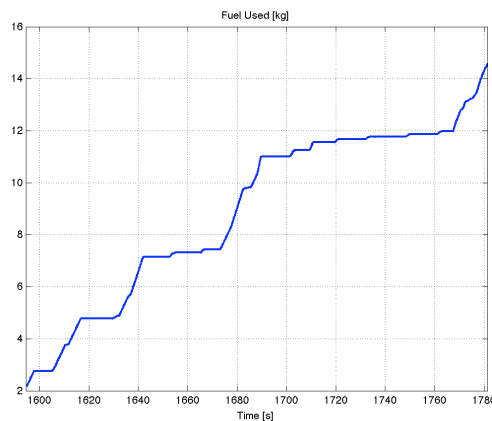


Figure 22. Fuel Used

## VI. CONCLUSIONS

This paper presented the concept for the Attitude Controller for the Exoatmospheric and Atmospheric Entry phase of the Mars Science Laboratory Entry, Descent and Landing. The controller is parameterized as 3 independent channels around the predicted trim position. Each channel controller is composed of a feedforward and a feedback path. The feedforward path enables fast response to large bank commands. The feedback path stabilizes the plant around attitude and rate deadbands while minimizing fuel usage. Feasibility and the satisfactory performance of this design have been demonstrated by computer simulations.

## ACKNOWLEDGEMENTS

The work was performed at the Jet Propulsion Laboratory, California Institute of Technology, under contract with the National Aeronautics and Space Administration.

© 2010 California Institute of Technology.  
Government sponsorship acknowledged.

## 7. REFERENCES

1. Brugarolas P.B., San Martin A.M., Wong E.C., "Mars Science Laboratory Entry Controller" AIAA GN&C Conference, Aug. 2008.
2. Mendeck G. F. and Carman G. L., "Guidance Design for Mars Smart Landers Using The Entry Terminal Point Controller" AIAA 2002-4502, August 2002.
3. Ingoldby R. N., "Guidance and Control System of the Viking Planetary Lander", Journal of Guidance and Control, Vol. 1, No. 3, 1978, pp. 189-196.
4. Holmberg N. A., Faust R. P., and Holt H. M. "Viking '75 Spacecraft Design and Test Summary" NASA Ref. Publ. 1027. November 1980.
5. "Viking Lander System Primary Mission Performance Report (Martin Marietta Corp.)", NASA CR-145148, April 1977.
6. Thurman S.W. and Flashner H., "Robust Digital Autopilot Design for Spacecraft Equipped with Pulse-Operated Thrusters". J. Guidance, Control and Dynamics, Vol. 19, No. 5, 1996, pp. 1047-1055.
7. Calhoun P. C. and Queen E. M., "Entry Vehicle Control System Design for the Mars Science Laboratory" Journal of Spacecraft and Rockets 2006 0022-4650 vol.43 no.2 (324-329)
8. Schoenenberger M., Cheatwood F., and Desai P., "Static Aerodynamics of the Mars Exploration Rover Entry Capsule" AIAA 2005-0056, January 2005.
9. Schoenenberger M., and Queen E.M., "Oscillation Amplitude Growth for a Decelerating Object with Constant Pitch Damping" AIAA 2006-6148, August 2006.